

Structural optimization using topological and shape  
sensitivity via a level set method\*

by

Grégoire Allaire<sup>1</sup>, Frédéric de Gournay<sup>1</sup>, François Jouve<sup>1</sup> and  
Anca-Maria Toader<sup>2</sup>

<sup>1</sup>Centre de Mathématiques Appliquées (UMR 7641), Ecole Polytechnique  
91128 Palaiseau, France  
e-mail: gregoire.allaire@polytechnique.fr  
e-mail: francois.jouve@polytechnique.fr

<sup>2</sup>CMAF, Faculdade de Ciências da Universidade de Lisboa  
Av. Prof. Gama Pinto 2, 1699 Lisboa, Portugal  
e-mail: amtan@ptmat.fc.ul.pt

**Abstract:** A numerical coupling of two recent methods in shape and topology optimization of structures is proposed. On the one hand, the level set method, based on the classical shape derivative, is known to easily handle boundary propagation with topological changes. However, in practice it does not allow for the nucleation of new holes (at least in 2-d). On the other hand, the bubble or topological gradient method is precisely designed for introducing new holes in the optimization process. Therefore, the coupling of these two methods yields an efficient algorithm which can escape from local minima in a given topological class of shapes. Both methods rely on the notion of gradient computed through an adjoint analysis, and have a low CPU cost since they capture a shape on a fixed Eulerian mesh. The main advantage of our coupled algorithm is to make the resulting optimal design largely independent of the initial guess.

**Keywords:** shape and topology optimization, level set method, topological gradient.

## 1. Introduction

This paper is a logical sequel of our previous work Allaire, Jouve, Toader (2002, 2004), where we proposed a numerical method of shape optimization based on

---

\*This work has been supported by the grant CNRS/GRICES *n*<sup>o</sup> 2002-12163 of the Centre National de la Recherche Scientifique (France) and the Gabinete de Relações Internacionais da Ciência e do Ensino Superior (Portugal).

the level set method and on shape differentiation. Indeed, in Allaire, Jouve, Toader (2002, 2004) we clearly indicated that, although the level set method makes possible topology changes during the optimization process, it does not solve the inherent problem of ill-posedness of shape optimization which manifests itself in the frequent existence of many local (non global) minima, usually having different topologies. The reason is that the level set method can easily remove holes but can not create new holes in the middle of a shape since the level set function obeys the maximum principle. In practice, this effect can be checked by varying the initialization which yields different optimal shapes with different topologies. To the best of our knowledge, other works on the level set method in shape optimization were also subject to this difficulty, see Osher, Santosa (2001), Sethian, Wiegmann (2000), Wang, Wang, Guo (2003). This absence of a nucleation mechanism is inconvenient mostly in 2-d: in 3-d, it is less important since holes can appear by pinching two boundaries (which can occur without destroying the connectivity of the structure).

In the present paper we propose as a remedy to couple our previous method with the topological gradient method of Schumacher, Masmoudi, Sokolowski and their co-workers (Eschenauer, Schumacher, 1994; C ea et al., 2000; Garreau, Guillaume, Masmoudi, 2001; Sokołowski,  ochowski, 1999, 2001). Roughly speaking the topological gradient method amounts to decide whether or not it is favorable (for decreasing the objective function) to nucleate a small hole in a given shape. As a matter of fact, creating a hole changes the topology and is thus one way of escaping local minima (due to topological constraint). Our coupled method of topological and shape gradients in the level set framework is therefore a great improvement (at least in 2-d) with respect to previous methods and is much less prone to finding local, non global, optimal shapes. In particular, for most of our 2-d numerical examples of compliance minimization, the expected global minimum is attained from the trivial full domain initialization. Nevertheless there are some (relatively few) examples of local minima if we choose a different initialization. For the 2-d mechanism design our coupled method is not fully independent of several parameters, including initialization, although it already produces excellent results with the trivial full domain initialization. To which extent the computed optimal shape depends on the initialization is presumably varying with the type of considered objective functions. As we already said, this improvement is far less important in 3-d where there is more geometrical freedom for the sole level set method, as confirmed by numerical experiments (see Allaire, Jouve, Toader, 2004, and the examples of Section 8). In practice, our 3-d numerical experiments for compliance minimization show that the optimal shapes are the same for the level set method with or without topological gradient (again, this may not be the case for other objective functions). In any case we do not claim that our coupled method is the ultimate one since local minima may still exist (even in the class of shapes sharing the same topology) and the speed of convergence can probably still be improved.

The main contribution of this paper is algorithmic and numerical. Actually, the theoretical tools used here have already been described (albeit separately) in the above quoted previous works. The novelty is in the coupling and in the robustness of the proposed numerical implementation. Our basic algorithm is to iteratively use the shape gradient or the topological gradient in a gradient-based descent algorithm. The tricks are to carefully monitor the decrease of the objective function (to avoid large changes in shape and topology) and to choose the right ratio of successive iterations in each method. We provide several 2-d and 3-d numerical examples for compliance minimization and mechanism design. In a slightly different context of inverse problems a different coupling of the shape and topological gradients (using the level set method too) has been proposed, Burger, Hackl, Ring (2004). There, the topological gradient was incorporated as a source term in the transport Hamilton-Jacobi equation used in the shape derivative algorithm for moving the shape. After this work was completed we learned that a similar method was developed independently in Wang, Yulin, Wang (2004).

## 2. Setting of the problem

In this paper we restrict ourselves to linear elasticity although there is no conceptual difficulty in extending our work to non-linear elasticity (see Allaire, Jouve, Toader, 2004). A shape is a bounded open set  $\Omega \subset \mathbb{R}^d$  ( $d = 2$  or  $3$ ) with a boundary made of two disjoint parts

$$\partial\Omega = \Gamma_N \cup \Gamma_D, \quad (1)$$

with Dirichlet boundary conditions on  $\Gamma_D$ , and Neumann boundary conditions on  $\Gamma_N$ . All admissible shapes  $\Omega$  are required to be a subset of a working domain  $D$  (a bounded open set of  $\mathbb{R}^d$ ). The shape  $\Omega$  is occupied by a linear isotropic elastic material with Hooke's law  $A$  defined, for any symmetric matrix  $\xi$ , by

$$A\xi = 2\mu\xi + \lambda(\text{Tr}\xi) \text{Id},$$

where  $\mu$  and  $\lambda$  are the Lamé moduli of the material. The displacement field  $u$  in  $\Omega$  is the solution of the linearized elasticity system

$$\begin{cases} -\text{div}(Ae(u)) = f & \text{in } \Omega \\ u = 0 & \text{on } \Gamma_D \\ (Ae(u))n = g & \text{on } \Gamma_N, \end{cases} \quad (2)$$

where  $f \in L^2(D)^d$  and  $g \in H^1(D)^d$  are the volume forces and the surface loads, respectively. Assuming that  $\Gamma_D \neq \emptyset$  (otherwise we should impose an equilibrium condition on  $f$  and  $g$ ), (2) admits a unique solution in  $u \in H^1(\Omega)^d$ .

The objective function is denoted by  $J(\Omega)$ . A first classical example is the compliance (the work done by the load)

$$J_1(\Omega) = \int_{\Omega} f \cdot u \, dx + \int_{\Gamma_N} g \cdot u \, ds = \int_{\Omega} Ae(u) \cdot e(u) \, dx, \quad (3)$$

which is very common in rigidity maximization. A second choice is a least square error between  $u$  and a target displacement

$$J_2(\Omega) = \left( \int_{\Omega} k(x) |u - u_0|^\alpha dx \right)^{1/\alpha}, \quad (4)$$

which is a useful criterion for the design of compliant mechanisms. We assume  $\alpha \geq 2$ ,  $u_0 \in L^\infty(D)$  and  $k \in L^\infty(D)$ , a non-negative given weighting factor. In both formulas (3) and (4),  $u = u(\Omega)$  is the solution of (2). We define a set of admissible shapes that must be open sets contained in the working domain  $D$  and of fixed volume  $V$

$$\mathcal{U}_{ad} = \left\{ \Omega \subset D \text{ such that } |\Omega| = V \right\}. \quad (5)$$

A model problem of shape optimization is

$$\inf_{\Omega \in \mathcal{U}_{ad}} J(\Omega). \quad (6)$$

In practice we rather work with an unconstrained problem. Introducing a Lagrange multiplier  $\ell$ , we consider the Lagrangian minimization

$$\inf_{\Omega \subset D} \mathcal{L}(\Omega) = J(\Omega) + \ell |\Omega|.$$

### 3. Shape derivative

In order to apply a gradient method to the minimization of (6) we recall the classical notion of shape derivative, going back to Hadamard (see e.g. Murat, Simon, 1976; Pironneau, 1984; Simon, 1980; Sokołowski, Zolesio, 1992). Starting from a smooth reference open set  $\Omega$ , we consider domains of the type

$$\Omega_\theta = (\text{Id} + \theta)(\Omega), \quad (7)$$

with  $\text{Id}$  the identity mapping from  $\mathbb{R}^d$  into  $\mathbb{R}^d$  and  $\theta$  a vector field in  $W^{1,\infty}(\mathbb{R}^d, \mathbb{R}^d)$ . It is well known that, for sufficiently small  $\theta$ ,  $(\text{Id} + \theta)$  is a diffeomorphism in  $\mathbb{R}^d$ . We remark that all admissible domains  $\Omega_\theta$  belong to the class of homotopy of the reference domain  $\Omega$  (it implies that in 2-d the number of connected components of the boundary remains constant). In other words, no change of topology is possible with this method of shape variation.

**DEFINITION 3.1** *The shape derivative of  $J(\Omega)$  at  $\Omega$  is defined as the Fréchet derivative in  $W^{1,\infty}(\mathbb{R}^d, \mathbb{R}^d)$  at  $\theta$  of the application  $\theta \rightarrow J((\text{Id} + \theta)(\Omega))$ , i.e.*

$$J((\text{Id} + \theta)(\Omega)) = J(\Omega) + J'(\Omega)(\theta) + o(\theta) \quad \text{with} \quad \lim_{\theta \rightarrow 0} \frac{|o(\theta)|}{\|\theta\|} = 0,$$

where  $J'(\Omega)$  is a continuous linear form on  $W^{1,\infty}(\mathbb{R}^d, \mathbb{R}^d)$ .

We recall the following classical result (see Allaire, Jouve, Toader, 2004, and references therein) about the shape derivatives for the two functionals under consideration: the compliance  $J_1$  (see (3)) and the least square error  $J_2$  (see (4)).

**THEOREM 3.1** *Let  $\Omega$  be a smooth bounded open set and  $\theta \in W^{1,\infty}(\mathbb{R}^d; \mathbb{R}^d)$ . Assume that the data  $f$  and  $g$  as well as the solution  $u$  of (2) are smooth, say  $f \in H^1(\Omega)^d$ ,  $g \in H^2(\Omega)^d$ ,  $u \in H^2(\Omega)^d$ . The shape derivative of (3) is*

$$J_1'(\Omega)(\theta) = \int_{\Gamma_N} \left( 2 \left[ \frac{\partial(g \cdot u)}{\partial n} + Hg \cdot u + f \cdot u \right] - Ae(u) \cdot e(u) \right) \theta \cdot n \, ds + \int_{\Gamma_D} Ae(u) \cdot e(u) \theta \cdot n \, ds \quad (8)$$

where  $H$  is the mean curvature defined by  $H = \operatorname{div} n$ . The shape derivative of (4) is

$$J_2'(\Omega)(\theta) = \int_{\Gamma_N} \left( \frac{C_0}{\alpha} k |u - u_0|^\alpha + Ae(p) \cdot e(u) - f \cdot p - \frac{\partial(g \cdot p)}{\partial n} - Hg \cdot p \right) \theta \cdot n \, ds + \int_{\Gamma_D} \left( \frac{C_0}{\alpha} k |u - u_0|^\alpha - Ae(u) \cdot e(p) \right) \theta \cdot n \, ds \quad (9)$$

where  $p$  is the adjoint state, assumed to be smooth, i.e.  $p \in H^2(\Omega)^d$ , defined as the solution of

$$\begin{cases} -\operatorname{div}(Ae(p)) &= -C_0 k(x) |u - u_0|^{\alpha-2} (u - u_0) & \text{in } \Omega \\ p &= 0 & \text{on } \Gamma_D \\ (Ae(p))n &= 0 & \text{on } \Gamma_N, \end{cases} \quad (10)$$

and  $C_0$  is a constant given by

$$C_0 = \left( \int_{\Omega} k(x) |u(x) - u_0(x)|^\alpha \, dx \right)^{1/\alpha-1}. \quad (11)$$

**REMARK 3.1** *The shape derivative of the volume constraint is easily computed. The result is*

$$V(\Omega) = \int_{\Omega} dx \quad \Rightarrow \quad V'(\Omega)(\theta) = \int_{\partial\Omega} \theta \cdot n \, ds.$$

#### 4. Topological derivative

One drawback of the previous method of shape derivative is that there is no change of topology in the parametrization  $\Omega_\theta$ . Numerical methods based on the

shape derivative may therefore fall into a local minimum (corresponding to the initial topology). Recently, a remedy to this inconveniency has been proposed as the bubble method, or topological asymptotic method, Eschenauer, Schumacher (1994), Garreau, Guillaume, Masmoudi (2001), Sokółowski, Żochowski (2001). The main idea is to test the optimality of a domain to topology variations by removing a small hole with appropriate boundary conditions.

We give a brief review of this method that we shall call in the sequel topological gradient method. Consider an open set  $\Omega \subset \mathbb{R}^d$  and a point  $x_0 \in \Omega$ . Introduce a fixed model hole  $\omega \subset \mathbb{R}^d$ , a smooth open bounded subset containing the origin. For  $\rho > 0$  we define the translated and rescaled hole

$$\omega_\rho = x_0 + \rho\omega.$$

Then we define the perforated domain

$$\Omega_\rho = \Omega \setminus \bar{\omega}_\rho. \quad (12)$$

The goal is to study the variations of the objective function  $J(\Omega_\rho)$  as  $\rho$  goes to 0. By insertion of a hole, the class of homotopy of  $\Omega_\rho$  is different from that of the limit domain  $\Omega$ . In particular, in 2-d the number of connected components of the boundary varies. Therefore, this method, which performs topology variations, is very different from the previous approach of shape derivative where the class of homotopy of  $\Omega_\rho$ , defined by (7), is always the same. In this respect, the two methods of topology differentiation and shape differentiation are essentially distinct. The corresponding sets of admissible domains have actually an empty intersection, even though both shape and topological derivatives rely on the adjoint method.

In the framework of structural optimization we put Neumann boundary conditions on  $\partial\omega_\rho$ . The objective function  $J(\Omega_\rho)$  is computed with the elastic displacement  $u_\rho$ , solution of the following elasticity problem

$$\begin{cases} -\operatorname{div}(Ae(u_\rho)) &= f & \text{in } \Omega_\rho \\ u_\rho &= 0 & \text{on } \Gamma_D \\ (Ae(u_\rho))n &= g & \text{on } \Gamma_N \\ (Ae(u_\rho))n &= 0 & \text{on } \partial\omega_\rho. \end{cases} \quad (13)$$

**DEFINITION 4.1** *If the objective function admits the following so-called topological asymptotic expansion for small  $\rho > 0$*

$$J(\Omega_\rho) = J(\Omega) + \rho^d D_T J(x_0) + o(\rho^d),$$

*then  $D_T J(x_0)$  is called the topological derivative at point  $x_0$ .*

Of course, since the topologies of  $\Omega_\rho$  and  $\Omega = \Omega_0$  are different, the objective function is not differentiable with respect to  $\rho$  or  $\rho^d$ , in the sense of the previous section.

The following result gives the topological derivative of the volume (or weight) of the domain  $\Omega$ . Note that this is a simple case where the functional does not depend on the state  $u$ .

LEMMA 4.1 *The topological derivative of  $V(\Omega) = \int_{\Omega} dx$  is*

$$D_T V(x) = -|\omega|.$$

From now on, we specify the model hole  $\omega$  to be the unit ball. This simplifies greatly the computations of the topological derivatives. However, note that the shape of the model hole  $\omega$  could also be optimized in order to find the "best" topological derivative, i.e. the smallest one if we minimize the objective function. The following two results give the expressions of the topological derivative for the compliance  $J_1(\Omega)$  (see (3)) and for the least square error  $J_2(\Omega)$  (see (4)) (for the proofs we refer to Garreau, Guillaume, Masmoudi, 2001; Sokolowski, Zochowski, 2001).

THEOREM 4.1 *Take  $\omega$  to be the unit ball of  $\mathbb{R}^d$ . Assume for simplicity that  $f = 0$  and that  $g$  as well as the solution  $u$  of (2) are smooth, say  $g \in H^2(\Omega)^d$ ,  $u \in H^2(\Omega)^d$ . For any  $x \in \Omega$  the topological derivative of  $J_1$  is, for  $d = 2$ ,*

$$D_T J_1(x) = \frac{\pi(\lambda + 2\mu)}{2\mu(\lambda + \mu)} \{4\mu Ae(u) \cdot e(u) + (\lambda - \mu)tr(Ae(u))tr(e(u))\}(x), \quad (14)$$

and for  $d = 3$ ,

$$D_T J_1(x) = \frac{\pi(\lambda + 2\mu)}{\mu(9\lambda + 14\mu)} \{20\mu Ae(u) \cdot e(u) + (3\lambda - 2\mu)tr(Ae(u))tr(e(u))\}(x). \quad (15)$$

A straightforward calculation shows that the topological derivatives in formulae (14) and (15) are nonnegative. This means that, for compliance minimization, there is no interest in nucleating holes if there is no volume constraint. However, if a volume constraint is imposed (see Lemma 4.1), the topological derivative may have negative values due to the addition of the term  $-\ell|\omega|$ , where  $\ell$  stands for the volume Lagrange multiplier.

THEOREM 4.2 *Take  $\omega$  to be the unit ball of  $\mathbb{R}^d$ . Assume for simplicity that  $f = 0$  and  $g$  as well as the solution  $u$  of (2) are smooth, say  $g \in H^2(\Omega)^d$ ,  $u \in H^2(\Omega)^d$ . For any  $x \in \Omega$  the topological derivative of  $J_2$  is, for  $d = 2$ ,*

$$D_T J_2(x) = -\frac{\pi}{\alpha} C_0 k(x) |u(x) - u_0(x)|^\alpha - \frac{\pi(\lambda + 2\mu)}{2\mu(\lambda + \mu)} \{4\mu Ae(u) \cdot e(p) + (\lambda - \mu)tr(Ae(u))tr(e(p))\}(x), \quad (16)$$

and for  $d = 3$ ,

$$D_T J_2(x) = -\frac{4\pi}{3\alpha} C_0 k(x) |u(x) - u_0(x)|^\alpha - \frac{\pi(\lambda + 2\mu)}{\mu(9\lambda + 14\mu)} \{20\mu A e(u) \cdot e(p) + (3\lambda - 2\mu) \text{tr}(A e(u)) \text{tr}(e(p))\}(x), \quad (17)$$

where  $p$  is the adjoint state, assumed to be smooth, i.e.  $p \in H^2(\Omega)^d$ , defined as the solution of (10), and  $C_0$  is the constant defined by (11).

The numerical application of the topological derivative is as follows. Consider the minimization of the Lagrangian

$$\mathcal{L}(\Omega) = J(\Omega) + \ell |\Omega|,$$

where  $\ell$  is a given Lagrange multiplier. The corresponding topological gradient is

$$D_T \mathcal{L}(x) = D_T J(x) - \ell |\omega|.$$

At the points  $x$  where  $D_T \mathcal{L}(x)$  is negative, we introduce holes into the current domain  $\Omega$ . Since this criterion applies for infinitesimal holes, we should not remove too much material. In practice it is better to nucleate holes only at the minimum (negative) points of this topological derivative. We remark that the application of the topological gradient can only decrease the volume of the current shape (see Nazarov, Sokolowski, 2004, for another criterion which amounts to adding a thin ligament).

## 5. Level set method for shape optimization

Consider  $D \subset \mathbb{R}^d$  a bounded domain in which all admissible shapes  $\Omega$  are included, i.e.  $\Omega \subset D$ . In numerical practice, the domain  $D$  will be uniformly meshed once and for all. We parameterize the boundary of  $\Omega$  by means of a level set function, following the idea of Osher and Sethian (1988). We define this level set function  $\psi$  in  $D$  such that

$$\begin{cases} \psi(x) = 0 & \Leftrightarrow x \in \partial\Omega \cap D, \\ \psi(x) < 0 & \Leftrightarrow x \in \Omega, \\ \psi(x) > 0 & \Leftrightarrow x \in (D \setminus \overline{\Omega}). \end{cases} \quad (18)$$

The normal  $n$  to the shape  $\Omega$  is recovered as  $\nabla\psi/|\nabla\psi|$  and the mean curvature  $H$  is given by the divergence of the normal  $\text{div}(\nabla\psi/|\nabla\psi|)$  (these quantities are computed throughout the whole domain  $D$ ).

During the optimization process, the shape  $\Omega(t)$  is going to evolve according to a fictitious time parameter  $t \in \mathbb{R}^+$  which corresponds to descent stepping.



The evolution of the level set function is governed by the following Hamilton-Jacobi transport equation (Osher and Sethian, 1988)

$$\frac{\partial \psi}{\partial t} + V|\nabla \psi| = 0 \quad \text{in } D, \quad (19)$$

where  $V(t, x)$  is the normal velocity of the shape's boundary. Equation (19) is simply obtained by differentiating the definition of a level set of  $\psi$ ,  $\psi(t, x(t)) = \text{Cst}$ , and replacing the velocity  $\dot{x}(t)$  by  $Vn$ .

The choice of the normal velocity  $V$  is based on the shape derivative computed in Theorem 3.1

$$\mathcal{L}'(\Omega)(\theta) = \int_{\partial\Omega} v\theta \cdot n \, ds, \quad (20)$$

where the integrand  $v(u, p, n, H)$  depends on the state  $u$ , adjoint state  $p$ , normal  $n$  and mean curvature  $H$ . The simplest choice is to take the steepest descent  $\theta = -vn$ . This yields a normal velocity for the shape's boundary  $V = -v$  (remark that  $v$  is given everywhere in  $D$  and not only on the boundary  $\partial\Omega$ ). Transporting  $\psi$  by (19) is equivalent to moving the boundary  $\partial\Omega$  (the zero level set of  $\psi$ ) along the descent gradient direction  $-\mathcal{L}'(\Omega)$ . The length of the time interval on which (19) is integrated corresponds to the descent step. It is not obvious that  $\theta = -vn$  belongs to  $W^{1,\infty}(\mathbb{R}^d, \mathbb{R}^d)$  in general (that depends on the regularity of  $\Omega$ ). This is one reason for choosing a different smoother velocity. Various formulas for  $V$  are possible and correspond to different choices of the inner product between  $\mathcal{L}'(\Omega)$  and  $\theta$ , or to a preconditioning of the gradient method (see e.g., Allaire, Jouve, Toader, 2004; Burger, 2003; Mohammadi, Pironneau, 2001).

The main point is that the Lagrangian evolution of the boundary  $\partial\Omega$  is replaced by the Eulerian solution of a transport equation in the whole fixed domain  $D$ . Likewise the elasticity equations for the state  $u$  (and for the adjoint state  $p$ ) are extended to the whole domain  $D$  by using the so-called ‘‘ersatz material’’ approach. It amounts to fill the holes  $D \setminus \Omega$  by a weak phase mimicking void but avoiding the singularity of the rigidity matrix. This is a well-known procedure in topology optimization which we already described in our previous work, Allaire, Jouve, Toader, 2004. In numerical practice, the weak material mimicking holes in  $D \setminus \Omega$  is chosen as  $10^{-3}A$ .

The Hamilton-Jacobi equation (19) is solved by an explicit second order upwind scheme (see e.g. Sethian, 1999) on a Cartesian grid. The boundary conditions for  $\psi$  are of Neumann type. Since this scheme is explicit in time, its time stepping must satisfy a CFL condition. In order to regularize the level set function (which may become too flat or too steep), we reinitialize it periodically by solving another Hamilton-Jacobi equation which admits as a stationary solution the signed distance to the initial interface, Sethian, 1999. In numerical practice, reinitialization is important because the level set function

often becomes too steep, which implies a bad approximation of the normal  $n$  or of the mean curvature  $H$ . For details of numerical implementation we refer to Allaire, Jouve, Toader (2004).

## 6. Optimization algorithm

For the minimization problem (6) we propose an iterative coupling of the level set method and the topological gradient method. Both methods are gradient-type algorithms, and so our coupled method can be cast into the framework of alternate directions descent algorithms.

The level set method relies on the shape derivative  $\mathcal{L}'(\Omega)(\theta)$  of Section 3, while the topological gradient method is based on the topological derivative  $D_T\mathcal{L}(x)$  of Section 4. These two types of derivative define independent descent directions that we simply alternate as follows.

In a first step, the level set function  $\psi$  is advected according to the velocity  $-v$  where  $v$  is the integrand in the shape derivative  $\mathcal{L}'(\Omega)$ , see (20). In a second step, holes are introduced into the current domain  $\Omega$  where the topological derivative  $D_T\mathcal{L}(x)$  is minimum and negative. More precisely, at those points we change the negative sign of the level set function  $\psi$  into a positive sign, according to the parametrization (18).

In practice, it is better to perform more level set steps than topological gradient steps. Therefore, the main parameter of our coupled algorithm is an integer  $n_{opt}$  which is the number of gradient steps between two successive application of the topological gradient (typically, the value of  $n_{opt}$  is 5 which means that 4 level set steps are performed for each topological gradient step). Our proposed algorithm is an iterative method, structured as follows:

1. Initialization of the level set function  $\psi_0$  corresponding to an initial guess  $\Omega_0$  (usually the full working domain  $D$ ).
2. Iteration until convergence, for  $k \geq 0$ :
  - (a) **Elasticity analysis.** Computation of the state  $u_k$  and adjoint state  $p_k$  through two problems of linear elasticity posed in  $\Omega_k$ . This yields the values of the shape derivative and of the topological gradient.
  - (b) **Shape gradient.** If  $\text{mod}(k, n_{top}) < n_{top}$ , the current shape  $\Omega_k$ , characterized by the level set function  $\psi_k$ , is deformed into a new shape  $\Omega_{k+1}$ , characterized by  $\psi_{k+1}$  which is the solution of the transport Hamilton-Jacobi equation (19) after a time interval  $\Delta t_k$  with the initial condition  $\psi_k$  and a velocity  $-v_k$  computed in terms of  $u_k$  and  $p_k$ . The time of integration  $\Delta t_k$  is chosen such that  $\mathcal{L}(\Omega_{k+1}) \leq \mathcal{L}(\Omega_k)$ .
  - (c) **Topological gradient.** If  $\text{mod}(k, n_{top}) = 0$ , we perform a nucleation step. We obtain a new shape  $\Omega_{k+1}$  by inserting new holes into the current shape  $\Omega_k$ . Namely, the sign of the level set function  $\psi_k$  is changed from negative to positive values (see (18)) in the regions

of  $\Omega_k$  where the topological derivative  $D_T\mathcal{L}_k$ , depending on  $u_k$  and  $p_k$ , has minimum negative values. If the objective function has increased, i.e. if  $\mathcal{L}(\Omega_{k+1}) > \mathcal{L}(\Omega_k)$ , then no holes are nucleated and we just take  $\Omega_{k+1} = \Omega_k$ .

For details about the shape gradient step, we refer to our previous work, Allaire, Jouve, Toader (2002, 2004). Let us simply recall that the time interval  $\Delta t_k$  plays the role of the descent step in the minimization of  $\mathcal{L}(\Omega)$ , and is usually one order of magnitude bigger than the explicit time step used for solving the Hamilton-Jacobi equation (19) (which is limited by the CFL condition). Since one explicit time step for (19) is much cheaper, in terms of CPU time and memory requirement, than solving the state equation (2) or adjoint state equation (10), for each single evaluation of  $u_k$  and  $p_k$  (that we call iteration) we perform many explicit time steps for the Hamilton-Jacobi equation.

The topological gradient step is performed only if the topological gradient is negative. If an infinitesimal small hole is inserted where  $D_T\mathcal{L}_k(x) < 0$ , then, by Definition 4.1 of the topological asymptotic, the objective function must decrease. However, in numerical practice, a hole can not be smaller than a single mesh cell, which is not so infinitesimally small. Even more, if the topological gradient  $D_T\mathcal{L}_k$  is negative in several touching cells, it amounts to remove from the current shape a large zone which is not small at all. For this reason, our algorithm has two additional parameters. First we never remove more than a given proportion of the total volume (typically we impose a bound of 1% at most in the decrease of the volume). Second, even if only few cells are removed, the objective function may increase because a single cell is too large. If it is the case, we do not accept the new nucleated holes and we simply keep the old shape,  $\Omega_{k+1} = \Omega_k$ . Nevertheless, such a decision may be too conservative: the shape of a cell (usually rectangular) is not optimal, the numerical evaluation of the topological gradient may be pessimistic because of discretization errors, and in any case, if a suboptimal hole is created the level set method will easily cancel it afterwards. Therefore, we accept the topological gradient step even if the objective function increases slightly. With introduction of a threshold parameter  $\epsilon_{gt}$  (typically 0.1), the new perforated shape is kept if

$$\mathcal{L}(\Omega_{k+1}) \leq (1 + \epsilon_{gt})\mathcal{L}(\Omega_k).$$

In our computer code, nucleating a hole in a cell means switching the sign of the level set function which has the effect of replacing in this cell the true material properties by those of the weak ersatz material. We always reinitialize the level set function after a hole nucleation in order that it becomes the signed distance to the shape boundary, Sethian (1999).

The choice of the coupling parameter  $n_{top}$  is more delicate since it has obviously some influence on the computed optimal shape. Recall that we perform  $n_{top}$  shape gradient steps between two topological gradient steps. If  $n_{top}$  is too small (say 1 or 2), then the objective function may not decrease smoothly and

the resulting shape may be very irregular. If  $n_{top}$  is too large, the level set method may have already converged to a local minimum where it is difficult to nucleate a new hole while decreasing the objective function. In most of our numerical examples we choose  $n_{top} = 5$ , but a different choice may yield a different final result. This is clearly a limitation of the method.

Finally, if we had chosen  $\epsilon_{gt} = 0$ , the objective function would always decrease and our algorithm would converge to a (local) minimum. At convergence, stability is attained in both optimization processes (shape and topology). In practice, for efficiency reasons (already explained) we take  $\epsilon_{gt} = 0.1$ , so the objective function does not always strictly decrease during a topological gradient step (in the hope to escape local minima) as can be checked on Figs. 2 and 6.

## 7. Numerical examples in 2-d

We begin with single loads, minimal compliance problems, i.e. we minimize the Lagrangian

$$\inf_{\Omega \subset D} \mathcal{L}(\Omega) = J_1(\Omega) + \ell|\Omega|$$

for a fixed positive Lagrange multiplier  $\ell > 0$ , and  $J_1$  being defined by (3). Our first example is the well-known cantilever problem which is fixed on the left wall and supports a unit vertical point load on the middle of the right wall. The working domain of size  $2 \times 1$  is discretized by 3200 squared elements. The Lagrange multiplier for the volume constraint is  $\ell = 100$ . For the sake of comparison we recall the result of our previous level set method based on shape gradient **without** topological gradient in Fig. 1.

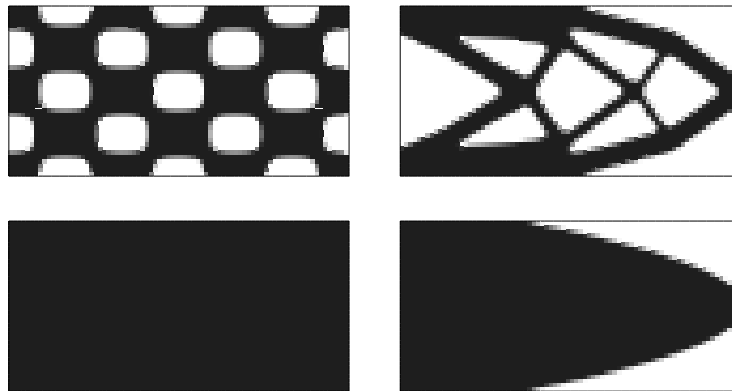


Figure 1. Shape gradient method (without topological derivative) for the cantilever problem: initializations (left) and optimal designs (right)

We choose two different initializations: the "best" one (i.e. yielding the global minimum), and the trivial one (without holes). Then, we run our new method with coupling parameter  $n_{top} = 5$ : namely, every 5 iterations of the shape gradient method we compute the topological derivative and nucleate new holes accordingly. We start from the trivial initial design with no holes in the working domain and perform 50 iterations. The result displayed on Fig. 2 is very similar to the best one in Fig. 1 and the objective function takes the same value. As we explained in Section 6, the choice of the coupling parameter  $n_{top}$  is very important (which is a default of the method). On Fig. 3 we obtain a suboptimal shape with less holes for a larger coupling parameter  $n_{top} = 10$ , and another suboptimal shape with irregular boundary for a smaller coupling parameter  $n_{top} = 1$  (implying that we perform only topological gradient steps).

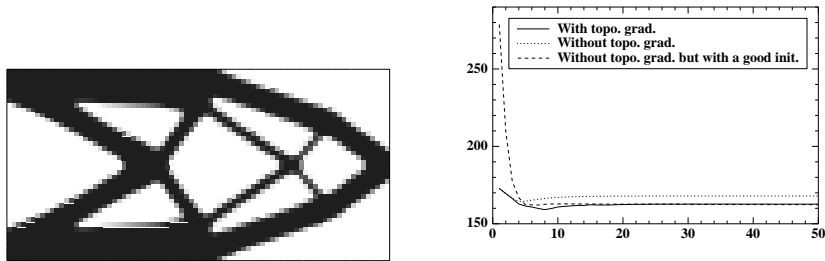


Figure 2. Coupled shape and topological gradient method for the cantilever: optimal design (left) and convergence history of the objective function (right)

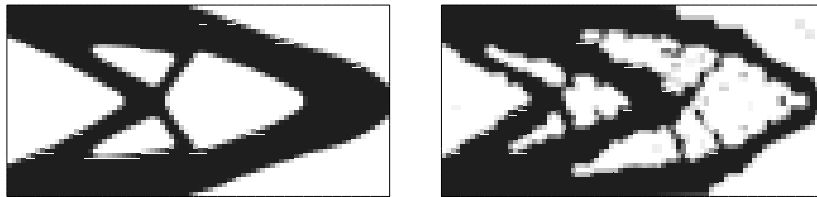


Figure 3. Optimal cantilever for the coupled shape and topological gradient method:  $n_{top} = 10$  (left) and  $n_{top} = 1$  (right)

The working domain of the bridge problem is a  $2 \times 1.2$  rectangle discretized with 3840 elements. The two lower corners have zero vertical displacement and a unit vertical load is applied at the middle of its bottom. The Lagrange multiplier is  $\ell = 22$ . The initialization is the full domain. The coupling parameter is  $n_{top} = 5$ . The final result as well as the intermediate results where new holes are nucleated by the topological gradient are displayed on Fig. 4.

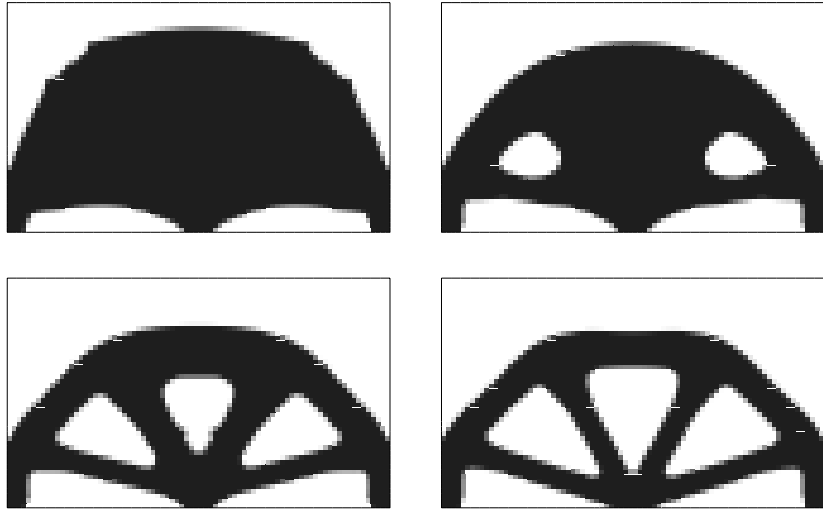


Figure 4. Optimal bridge in 2-d: iterations 6, 11, 16 and 100

This bridge problem is an example where local minima still exist despite the use of the topological gradient (with fixed value of the coupling parameter  $n_{top}$ ). Indeed, we run the same numerical example with a different initialization, namely the lower half of the domain. The resulting optimal shape, displayed on Fig. 5, is better as can be checked on Fig. 6.

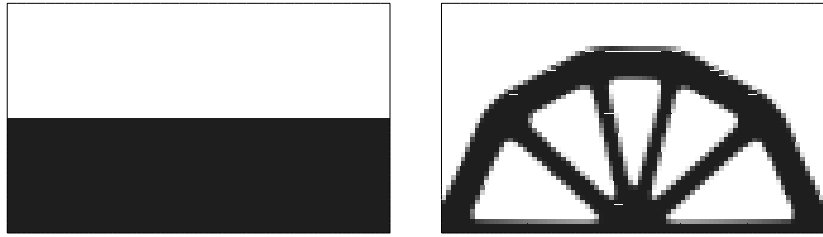


Figure 5. Optimal bridge in 2-d: half domain initialization and optimal shape after 100 iterations

For the optimal mast problem, we use a T-shaped working domain with height 6, width 2 at the bottom and 4 at the top. The two lower corners are fixed while two loads are applied at the lower corners of the horizontal branch of the T (see Fig. 8). The quadrangular mesh is made of 3600 square cells. The Lagrange multiplier for the weight is equal to 15. The initialization is the full

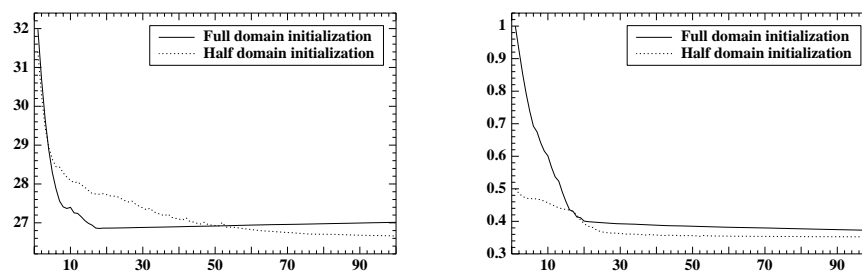


Figure 6. Convergence history of the objective function (left) and of the weight (right) for the 2-d optimal bridge

domain. We run 100 iterations of the level set method with coupling parameter  $n_{opt} = 5$ . The first topological gradient step occurs after iteration 5 where a hole is created in the upper part of the structure. Other holes are nucleated after iterations 10 and 15 and allow for a noticeable decrease of the objective function. However, the hole nucleated after iteration 20 is not so favorable and disappears in the final optimal result. The convergence is smooth except for small peaks in the objective function after each topological gradient step (see Fig. 7).

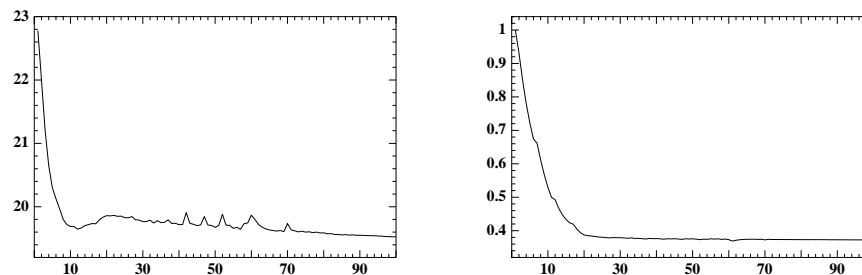


Figure 7. Convergence history of the objective function (left) and of the weight (right) for the 2-d optimal mast of Fig. 8

We now turn to mechanism design, i.e. we minimize the Lagrangian

$$\inf_{\Omega \subset D} \mathcal{L}(\Omega) = J_2(\Omega) + \ell |\Omega|$$

for a fixed Lagrange multiplier  $\ell$ , and  $J_2$  being defined by (4) with the exponent  $\alpha = 2$ . The first example is a negative Poisson ratio mechanism: when we pull on the lateral sides it expands vertically. By symmetry, only 1/4 of the whole domain (of size  $2 \times 2$ ) is meshed by  $80 \times 80$  squared cells. All sides are made

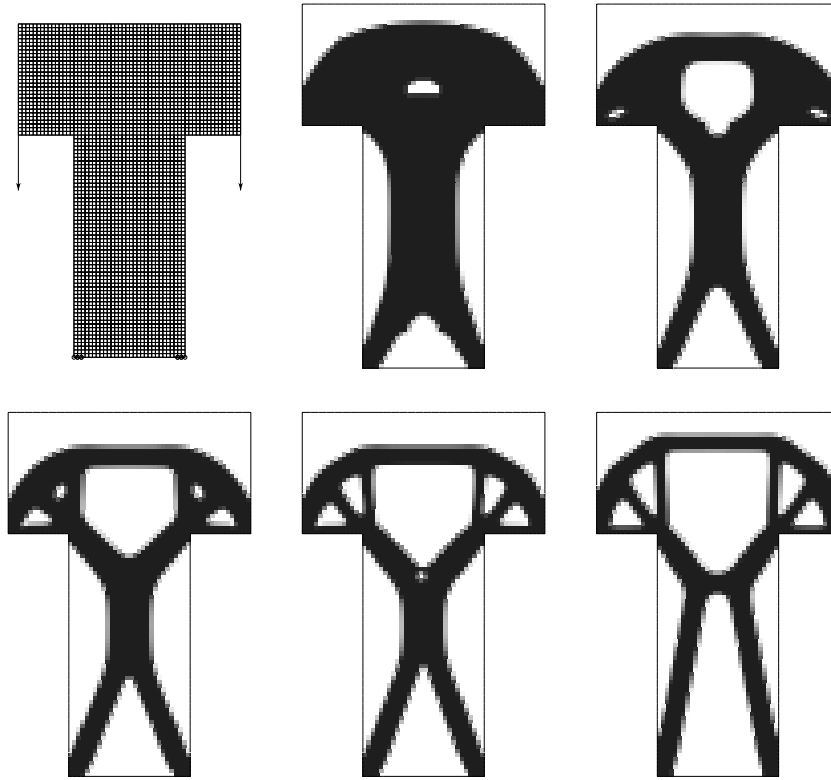


Figure 8. Optimal mast in 2-d: boundary conditions and iterations 6, 11, 16, 21 and 100

of a stiff material and excluded from optimization. In the formula for  $J_2$ , the localization coefficient  $k(x)$  is non-zero (equal to 1) only at the boundary and the target displacement  $u_0$  is  $(0, 1)$  on the top boundary,  $(0, -1)$  on the bottom one and  $(0, 0)$  on the lateral ones. The Lagrange multiplier is  $\ell = 0$ . Starting from a full domain initialization we perform 500 iterations with the coupling parameter  $n_{top} = 15$  (see Fig. 9). As usual, the convergence is slower than for compliance minimization (see Fig. 10). Furthermore, the computed optimal design is very sensitive to all parameters of the algorithm including the stiffness ratio between the weak ersatz material and the true material (which is here equal to  $10^{-2}$ ), the coupling parameter  $n_{top}$ , and the initialization. Different choices of these parameters lead to different topologies with similar performances.

Our second example is a gripping mechanism. Fig. 11 shows the boundary conditions and the target displacement. A small force, parallel to the target displacement in the opposite direction, is also applied on the jaws of the me-



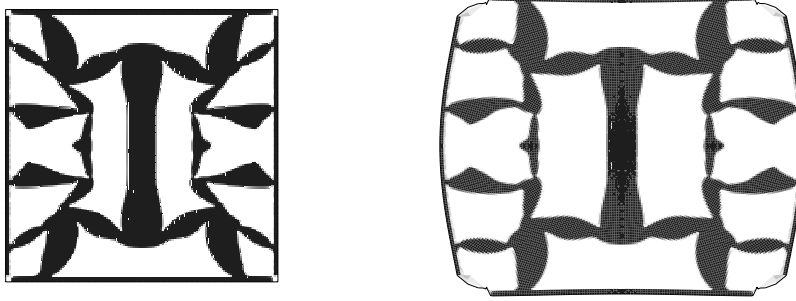


Figure 9. Optimal design (left) for the negative Poisson ratio mechanism, and deformed configuration (right)

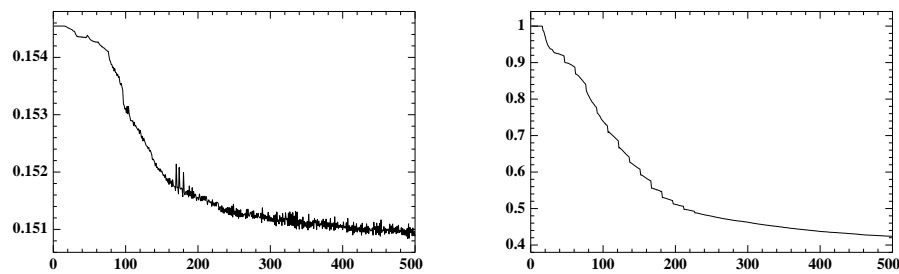


Figure 10. Convergence history of the objective function (left) and of the weight (right) for the negative Poisson ratio mechanism

chanism in order to simulate a reaction force. We also add a constraint that the displacement of the location of the input forces are not too large. Starting from a full domain initialization we perform 300 iterations with the coupling parameter  $n_{top} = 5$  (see Fig. 12). The resulting optimal design is very similar to those obtained by the level set method, Allaire, Jouve, Toader (2004), or the homogenization method, Allaire (2001).

**REMARK 7.1** *In all our examples the volume was not fixed. Rather, for a fixed Lagrange multiplier, we minimized the Lagrangian  $\mathcal{L}(\Omega) = J(\Omega) + \ell|\Omega|$ . The reason is that we want to use a trivial initialization which do not bias the result. If we have to respect a volume constraint, the initial shape must include holes and the location and shapes of those holes may influence the result. Of course, it is not difficult to update the Lagrange multiplier  $\ell$  to satisfy a volume constraint, Allaire, Jouve (2005).*

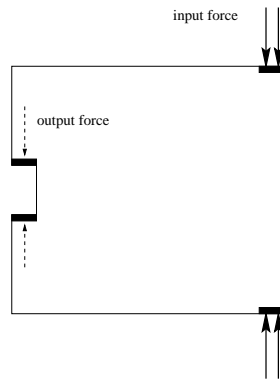


Figure 11. Boundary conditions and target displacement for the gripping mechanism

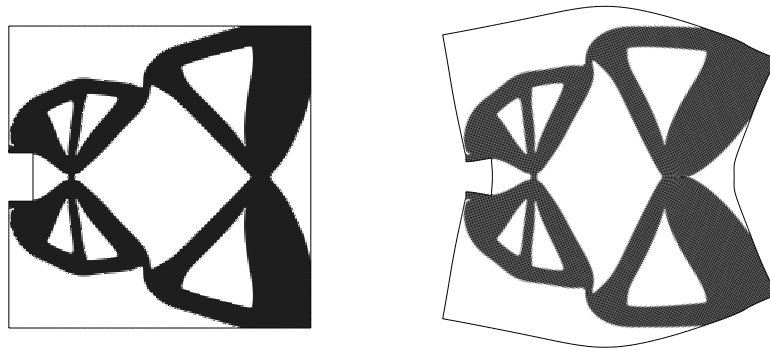


Figure 12. Optimal design (left) for the gripping mechanism, and deformed configuration (right)

## 8. Numerical examples in 3-d

As we already said, the level set method works better in 3-d than in 2-d because holes are easier to create in 3-d, Allaire, Jouve, Toader (2004). In all our 3-d numerical experiments, incorporating the topological gradient did not help in finding better optimal shapes. Of course, it may happen that the topological gradient speed up a little the convergence process but this effect is not striking and was not systematically studied here. We begin with compliance minimization problems.

We first optimize a 3-d cantilever where the right side is fixed and a horizontal unit point load is applied at the middle of the left side (see Fig. 13). The working

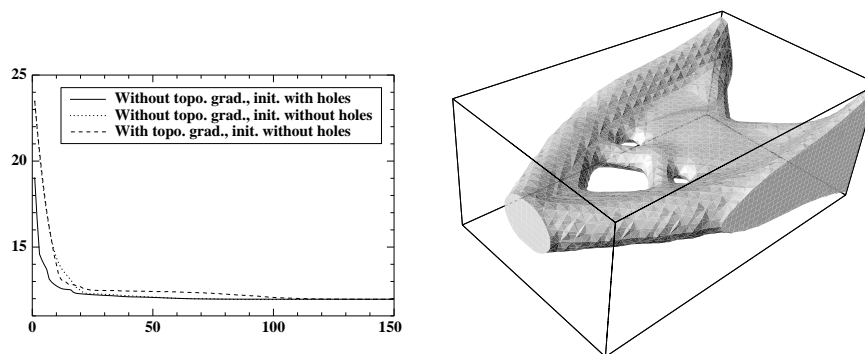


Figure 13. Optimal cantilever in 3-d (right). Convergence history of the objective function (left).

domain is of size  $3 \times 2 \times 5$  and only half of it is discretized (by symmetry) using 15000 quadrilateral elements. The Lagrange multiplier for the weight constraint is  $\ell = 20$ . The coupling parameter is  $n_{top} = 5$ . We obtain precisely the same optimal shape with the level set method and our coupled method (incorporating the topological gradient). More than that, the result of the level set method was the same for two different initializations: either we start from the full working domain (without holes) or from a periodic collection holes as in Allaire, Jouve, Toader (2004). We believe that for any non-pathologic initialization we always get the same optimal shape. Finally, the result of our coupled method is also independent of the parameter  $n_{top}$  which characterizes the number of level set iterations between two evaluations of the topological gradient.

The same conclusions can be drawn from the 3-d optimal mast example (see Fig. 14). Its result is independent of the method and of the initialization. We tried other simple examples in 3-d that confirm this behavior. Therefore, in view of this (limited) number of numerical experiments, we believe the level set method alone in 3-d is as good as the coupled method (level set plus topological gradient).

## 9. Conclusion

We have proposed a coupled method of shape and topology differentiation in the level set framework. It is an iterative algorithm where repeatedly the shape boundary evolves smoothly and new small holes are nucleated. In 2-d numerical practice, this method is more insensitive to the initialization and is thus a great improvement over the previous level set method (at least for compliance minimization). In 3-d, our numerical experiments show that the improvement is not sensitive since the optimal shapes are the same than those obtained by the level set method (at least for compliance minimization).

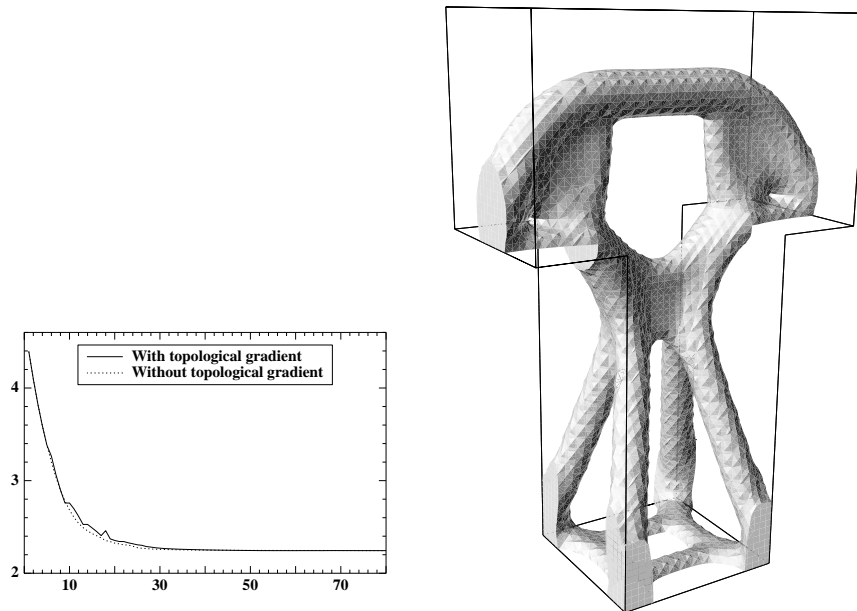


Figure 14. Optimal mast in 3-d (right). Convergence history of the objective function (left).

There is still some room for improvement in the following directions: first, extend and test the robustness of our method for more general objective functions, second increase the speed of convergence, third implement a recent idea of Nazarov and Sokolowski (2004) for another type of topology variations. Indeed, removing a hole in a shape is not the only possibility for changing the topology. Another issue, investigated in Nazarov and Sokolowski (2004), is to add a thin ligament between two separated boundaries of the shape. It is somehow the opposite process of hole perforation, since it adds some material to the shape. Numerically this could be an interesting process that may avoid, for example, the two different optimal shapes obtained for the 2-d bridge problem.

Finally, we remark that, for compliance minimization problems, the homogenization method, Allaire (2001), Bendsøe (1995), Bendsøe, Sigmund (2003), is still the most reliable method since it is the only one which is fully independent of the initialization and free of any important parameters.

## References

ALLAIRE, G. (2001) *Shape Optimization by the Homogenization Method*. Springer Verlag, New York.

- ALLAIRE, G. and JOUVE, F. (2005) A level-set method for vibration and multiple loads structural optimization. To appear in *Comput. Methods Appl. Mech. Engrg.*
- ALLAIRE, G., JOUVE, F. and TOADER, A.-M. (2002) A level set method for shape optimization. *C. R. Acad. Sci. Paris, Série I*, **334**, 1125-1130.
- ALLAIRE, G., JOUVE, F. and TOADER, A.-M. (2004) Structural optimization using sensitivity analysis and a level set method, *J. Comp. Phys.* **194** (1), 363-393.
- BENDSØE, M. (1995) *Methods for Optimization of Structural Topology, Shape and Material*. Springer Verlag, New York.
- BENDSØE, M. and SIGMUND, O. (2003) *Topology Optimization. Theory, Methods, and Applications*. Springer Verlag, New York.
- BURGER, M. (2003) A framework for the construction of level set methods for shape optimization and reconstruction. *Interfaces and Free Boundaries* **5**, 301-329.
- BURGER, M., HACKL, B. and RING, W. (2004) Incorporating topological derivatives into level set methods. *J. Comp. Phys.* **194** (1), 344-362.
- CÉA, J., GARREAU, S., GUILLAUME, P. and MASMOUDI, M. (2000) The shape and topological optimizations connection. *IV WCCM*, Part II (Buenos Aires, 1998), *Comput. Methods Appl. Mech. Engrg.* **188**, 713-726.
- ESCHENAUER, H. and SCHUMACHER, A. (1994) Bubble method for topology and shape optimization of structures. *Structural Optimization* **8**, 42-51.
- GARREAU, S., GUILLAUME, P. and MASMOUDI, M. (2001) The topological asymptotic for PDE systems: the elasticity case. *SIAM J. Control Optim.* **39** (6), 1756-1778.
- MOHAMMADI, B. and PIRONNEAU, O. (2001) *Applied Shape Optimization for Fluids*. Clarendon Press, Oxford.
- MURAT, F. and SIMON, S. (1976) Etudes de problèmes d'optimal design. *Lecture Notes in Computer Science 41*, Springer Verlag, Berlin, 54-62.
- NAZAROV, S.A. and SOKOŁOWSKI, J. (2004) The topological derivative of the Dirichlet integral under formation of a thin ligament. *Siberian Math. J.* **45**, 341-355.
- OSHER, S. and SANTOSA, F. (2001) Level set methods for optimization problems involving geometry and constraints: frequencies of a two-density inhomogeneous drum. *J. Comp. Phys.* **171**, 272-288.
- OSHER, S. and SETHIAN, J.A. (1988) Front propagating with curvature dependent speed: algorithms based on Hamilton-Jacobi formulations. *J. Comp. Phys.* **78**, 12-49.
- PIRONNEAU, O. (1984) *Optimal Shape Design for Elliptic Systems*. Springer-Verlag, New York.
- SETHIAN, J.A. (1999) *Level Set Methods and Fast Marching Methods: Evolving Interfaces in Computational Geometry, Fluid Mechanics, Computer Vision and Materials Science*. Cambridge University Press.

- SETHIAN, J. and WIEGMANN, A. (2000) Structural boundary design via level set and immersed interface methods. *J. Comp. Phys.* **163**, 489-528.
- SIMON, J. (1980) Differentiation with respect to the domain in boundary value problems. *Num. Funct. Anal. Optimz.* **2**, 649-687.
- SOKOŁOWSKI, J. and ŻOCHOWSKI, A. (1999) On the topological derivative in shape optimization. *SIAM J. Control Optim.* **37**, 1251-1272.
- SOKOŁOWSKI, J. and ŻOCHOWSKI, A. (2001) Topological derivatives of shape functionals for elasticity systems. *Mech. Structures Mach.* **29** (3), 331-349.
- SOKOŁOWSKI, J. and ZOLESIO J.P. (1992) *Introduction to Shape Optimization: Shape Sensitivity Analysis*. Springer Series in Computational Mathematics **10**, Springer, Berlin.
- WANG, M.Y., WANG, X. and GUO, D. (2003) A level set method for structural topology optimization. *Comput. Methods Appl. Mech. Engrg.* **192**, 227-246.
- WANG, X., YULIN, M. and WANG, M.Y. (2004) Incorporating topological derivatives into level set methods for structural topology optimization. In: T. Lewinski et al., eds., *in Optimal shape design and modeling*, Polish Academy of Sciences, Warsaw, 145-157.